

# Breath Level Acetone Discrimination Through Temperature Modulation of a Hierarchical ZnO Gas Sensor

Jiaqi Chen<sup>1</sup>, Xiaofang Pan<sup>5</sup>, Farid Boussaid<sup>2,\*</sup>, Allan McKinley<sup>3</sup>, Zhiyong Fan<sup>1,\*</sup>,  
and Amine Bermak<sup>1,4,\*\*</sup>

<sup>1</sup>Department of Electronic and Computer Engineering, Hong Kong University of Science and Technology, Hong Kong

<sup>2</sup>School of Electrical, Electronic and Computer Engineering, University of Western Australia, Perth, WA 6009, Australia

<sup>3</sup>School of Molecular Sciences, University of Western Australia, Perth, WA 6009, Australia

<sup>4</sup>College of Science and Engineering, Hamad Bin Khalifa University, Doha 3263, Qatar

<sup>5</sup>College of Information Engineering, Shenzhen University, Shenzhen 518060, China

\*Senior Member, IEEE

\*\*Fellow, IEEE

Manuscript received August 2, 2017; revised August 11, 2017; accepted August 11, 2017. Date of publication August 15, 2017; date of current version August 29, 2017.

**Abstract**— A hierarchical ZnO nanostructure gas sensor was fabricated to evaluate the concentration of acetone in exhaled human breath. Such information can be used for the diagnosis of diabetes since acetone levels in exhaled breath in excess of 1.8 ppm are typically associated with diabetes sufferers. When exposed to acetone, the fabricated sensor exhibits a unique U-shaped response curve as a function of temperature. It was discovered that its acetone sensing behavior changes from oxidizing to reducing as the temperature increases. The sensor's characteristic response was shown to be associated to the carbonyl group present in the acetone molecule. The fabricated hierarchical ZnO nanostructure sensor is able to detect acetone concentration levels as low as 1 ppm even at room temperature, making it suitable for noninvasive diabetes diagnosis.

**Index Terms**—Sensor materials, diabetes, acetone detection, breath analysis, ZnO hierarchical nanostructure, gas sensors.

## I. INTRODUCTION

Gas sensors have found a wide range of applications from air quality monitoring, detection of toxic gases and explosives, food quality monitoring to medical diagnosis through breath analysis [1], [2]. In the case of diabetes, which is known to cause a distinct sweet and fruity odor in the breath of sufferers, a number of studies have shown that it can be diagnosed by evaluating the concentration of acetone in exhaled breath. This constitutes a simple, low cost and noninvasive approach to diagnose diabetes in the general population as only a gas sensor would be required. However, such a device would need to be highly sensitive since acetone concentration levels are in the order of parts per million (ppm) for both healthy subjects (<0.76 ppm) and diabetes sufferers (>1.8 ppm) [3]. In addition, the sensor needs to be highly selective as human breath comprises in excess of 3500 different chemical species.

A range of sensing materials (e.g.,  $K_2W_7O_{22}$ , ZnO and  $WO_3$ ) have been developed for acetone detection [4]–[8]. However, these sensors exhibit low sensitivity while requiring operation at high temperature. In addition, such sensors have limited discrimination capability given that, at high temperatures, the reducing response associated to acetone is similar to that of other reducing gases like CO and ethanol. This greatly complicates the acetone detection process and makes it very dependent on the classification accuracy of advanced post signal processing algorithms [9]–[11]. To address these limitations, we

propose to achieve selective acetone detection through temperature modulation of a hierarchical ZnO nanostructure gas sensor. The proposed approach provides a unique U-shaped fingerprint for acetone detection in human breath. In addition, it provides a high performance and low cost diabetes diagnosis solution through the large surface-to-volume ratio of the sensor's nanocomb structure and its compatibility with industry standard fabrication processes.

## II. EXPERIMENTAL

A hierarchical ZnO gas sensor was fabricated using only standard Micro-Electro-Mechanical Systems (MEMS) and Chemical Vapor Deposition (CVD) processes [12]. The “solution-free” process adopted avoids the ultrasonic damage and the random distribution of ZnO nanowires associated to the traditional time-consuming “drop-cast” method [12]. The fabrication process can be summarized as follows. A silicon wafer coated with a 1- $\mu$ m thick silicon dioxide passivation layer is first prepared. A layer of photoresist (HPR 504) is then spin-coated on top of the wafer. A cross-finger-shape mask is used in the subsequent UV exposure. This is followed by development in a FHD-5 solution (1 min) to expose the electrodes' region. Next, 20 nm-Ti and 80 nm-Pt layers are sputtered onto the exposed region to form ohmic contacts with the ZnO nanostructure. Finally, a 20 nm-Au layer is sputtered to act as the catalyst for ZnO growth. After photoresist removal, a conical vial was placed in the CVD glass tube with 400 mg of Zn powder (99.9% from Sigma-Aldrich Inc.) in the windward side of the cone and the patterned silicon substrate in the leeward side. A flow of a mixture of oxygen and argon in a volume ratio of 1:49 was used to optimize the nucleation process at 700 °C for 30 min.

Corresponding Author: Jiaqi Chen (e-mail: jchenbd@connect.ust.hk). (Jiaqi Chen and Xiaofang Pan contributed equally to this work.)

Associate Editor: J. M. Corres.

Digital Object Identifier 10.1109/LENS.2017.2740222

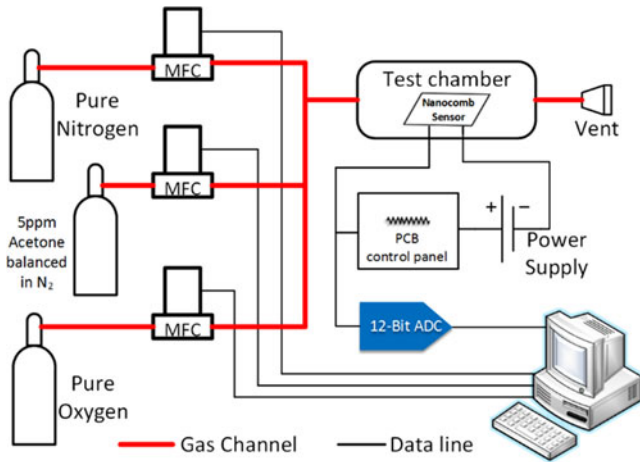


Fig. 1. Overview of the experimental testing setup.

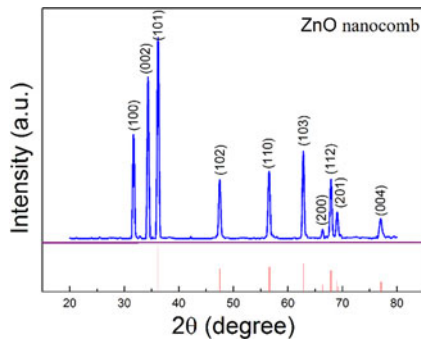


Fig. 2. XRD pattern of the hierarchical ZnO nanocombs.

The structure and morphology of the fabricated sensor was examined by X-ray diffraction (XRD, PW1830 (Philips)) and scanning electron microscopy (SEM, JEOL-7100F).

### III. TEST SETUP

The testing setup is presented in Fig. 1. Computer-controlled Mass Flow Controllers (MFCs) on gas channels maintain a total flow rate of 500 standard-state cubic centimeters per minute (sccm) for synthetic air with a constant oxygen ratio of 20%. Each measurement involves heating the sensor at the correct temperature before subsequent exposures to synthetic air (30 min) and acetone (15 min). The testing chamber is a glass bottle exhibiting an input end and a vent end; which is used to maintain a standard atmospheric pressure inside the chamber. The resistance of the ZnO hierarchical gas sensor was readout using a constant resistor connected in series, with a constant applied voltage. Sensed voltages were read out using a 12-bit analog to digital converter (ADC).

### IV. RESULTS AND DISCUSSION

The X-ray diffraction pattern of the final device shown in Fig. 2 matches well with the powder pattern for ZnO JCPDS card (no.36-1451), indicating the sensor is composed of ZnO in the wurzite structure. Fig. 3 shows an SEM image of the fabricated hierarchical ZnO gas sensor, which appears as a nanocomb with a shaft and teeth

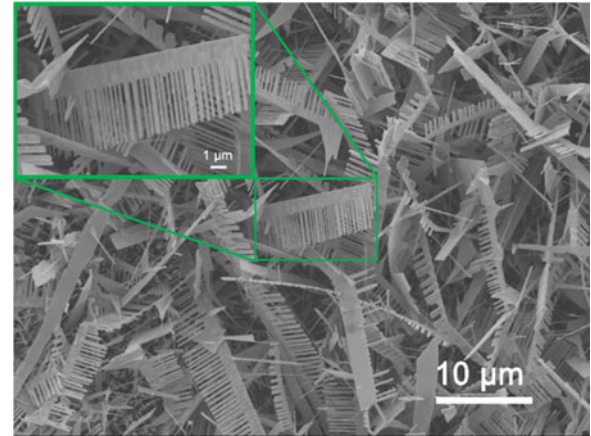


Fig. 3. SEM image of hierarchical ZnO nanocombs.

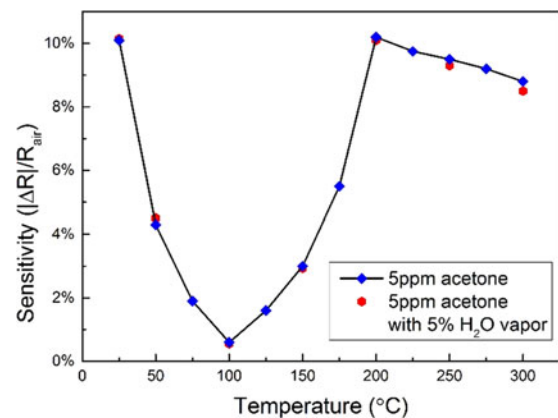


Fig. 4. Sensitivity of the hierarchical ZnO nanocomb sensors towards 5 ppm acetone (in dry air and 5% humidity) as a function of operating temperature in the range of 25 °C to 300 °C.

sections. The width of the shaft region ranges from a few hundred nanometers to 1- $\mu$ m while the height of the teeth is around 2.2- $\mu$ m.

The sensor was also characterized using the testing setup described in [13]. Experiments have been conducted to evaluate the response of the fabricated gas sensor at temperatures ranging from 25 °C to 300 °C and for acetone concentration levels ranging from 1 ppm to 5 ppm in dry air and 5% humidity. Note that the testing setup does not permit characterization of the sensor at sub-ppm levels.

Fig. 4 shows the sensor sensitivity to 5 ppm of acetone from room temperature 25 °C to 300 °C under atmosphere pressure and no infrared light, with the sensitivity defined as

$$|\Delta R|/R_{\text{air}} = |R_g - R_{\text{air}}|/R_{\text{air}} \quad (1)$$

and  $R_g$  and  $R_{\text{air}}$  representing the sensor resistances when exposed to acetone and dry air, respectively. Fig. 4 shows that a unique U-shaped graph is observed for the sensor response to acetone as a function of temperature, with the maximum sensitivity observed at 25 °C and 200 °C. The gas sensitivity  $|\Delta R|/R_{\text{air}}$  is seen to be around 10% at 25 °C and 200 °C, with  $\Delta R (= R_g - R_{\text{air}})$  positive at 25 °C and negative at 200 °C. In addition, we have conducted acetone measurements in the presence of 5% humidity, which corresponds to the level of humidity found in human breath. Experimental results are plotted as red dots in

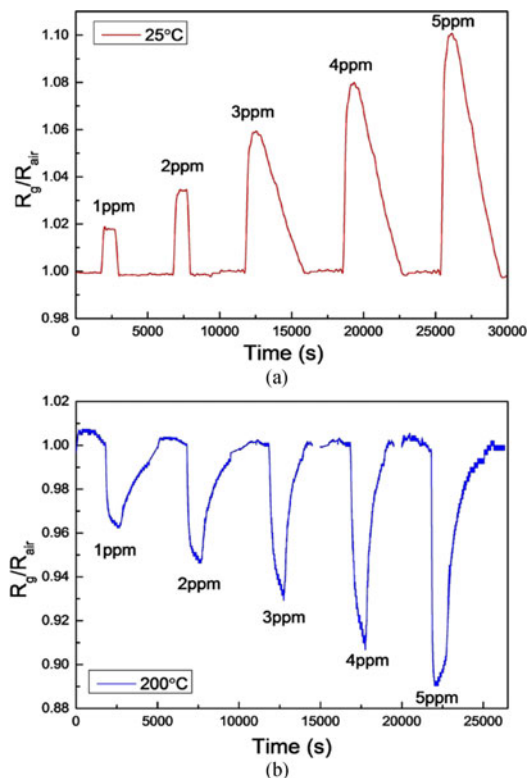


Fig. 5. Dynamic response of the hierarchical ZnO sensor towards acetone with different concentrations ranging from 1–5 ppm at (a) 25 °C and (b) 200 °C.

Fig. 4 for different operating temperatures. The influence of humidity is seen to be negligible.

Fig. 5(a) and (b) report the sensor responses at these temperatures for acetone concentration levels increasing from 1 to 5 ppm, with a 1 ppm step. In the two graphs, the gas sensor response is defined as  $R_g/R_{air}$ , where  $R_g$  and  $R_{air}$  refer to the sensor resistance when exposed to the target gas mixture and to dry air, respectively. The response time to 1 ppm acetone was found to be 190 s at room temperature and 398 s at 200 °C. The corresponding recovery times are 280 s at room temperature and 2228 s at 200 °C. Multiple gas sensors operating simultaneously at different operating temperatures could be used to achieve fast acetone discrimination.

At room temperature Fig. 5(a), the sensor resistance is seen to increase when exposed to acetone-air mixtures while at high temperature the resistance falls. This decrease at high temperature (420 °C)—for an n-type gas sensor exposed to acetone—has been previously reported [6]. It is due to the oxidation of acetone—when exposed to air—into carbon monoxide, carbon dioxide and water, which results in the subsequent release of additional free electrons into the conduction band of the ZnO. The observed resistance increase (Fig. 5(a)) at room temperature has also been reported by Long *et al.* [14]. They ascribed this phenomenon to the reduction of the electron mean free path, as a result of target gas adsorption. A recent Fourier transform infrared spectroscopy (FTIR) and theoretical study of acetone adsorption onto a ZnO surface under ultrahigh vacuum conditions also reported the behaviour of acetone absorbed onto ZnO at room temperature [15]. They showed that the absorbed acetone rearranged to an enolate and transferred a hydrogen to the surface, which caused a polarity change

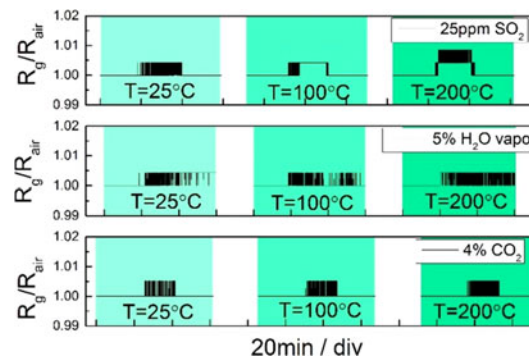


Fig. 6. Response of the sensor towards SO<sub>2</sub>, humidity, and CO<sub>2</sub> at different temperatures.

of the surface [15]. Unlike acetone, other gases found in human breath (e.g., oxygen, nitrogen, carbon monoxide, carbon dioxide, water vapor, argon or hydrogen) do not exhibit an oxidizing or reducing behavior that is dependent on temperature [9]–[11], [16]. This observation suggests that analyzing the sensor’s response as a function of temperature (Fig. 4) can provide a means to uniquely distinguish acetone in exhaled human breath.

To demonstrate the sensor’s selectivity in the presence of interfering gases present in human breath, we have evaluated its response towards SO<sub>2</sub>, CO<sub>2</sub>, and H<sub>2</sub>O at concentrations of 25 ppm, 4%, and 5%, respectively. For CO<sub>2</sub> and H<sub>2</sub>O, the concentrations were chosen to be similar to that found in human breath. However, for SO<sub>2</sub>, the concentration was chosen much higher to further evaluate the selectivity of the sensor towards acetone. In addition, experiments were conducted at three different temperatures (25 °C, 100 °C, 200 °C) to determine the impact of temperature modulation on the sensor response to these gases. The normalized responses  $R_g/R_{air}$  of the sensor to SO<sub>2</sub>, CO<sub>2</sub>, and H<sub>2</sub>O are shown in the above Fig. 6. The injection of SO<sub>2</sub>, H<sub>2</sub>O or CO<sub>2</sub> is seen to result in  $R_g/R_{air}$  changes of the order of the quantization error of the ADC. The acquired response curves show that the sensitivity ( $|\Delta R/R$ ) of the sensor towards these interfering gases is less than 0.4% compared to 10% for acetone. In addition, in the presence of 5% humidity, the sensitivity of the sensor exhibits slight changes (Fig. 4) given the relatively low level of humidity found in human breath. Note that, below 100 °C, both acetone and H<sub>2</sub>O exhibit an oxidizing behavior, resulting in a slight sensitivity increase. In contrast, above 100 °C, acetone exhibits a reducing behavior while H<sub>2</sub>O still exhibits an oxidizing behavior, leading to a slight sensitivity decrease (Fig. 4). These different acquired results show that the proposed sensor still exhibits high selectivity towards acetone in the presence of interfering gases.

Fig. 7 illustrates the process of adsorption of acetone at different temperatures. Note that the oxygen atom in the carbonyl group of acetone is polarized and has a net negative charge [17]. Following chemical adsorption, the oxygen binds to a positively charged zinc atom on the surface of the sensor affecting the mobility of the conduction band electrons and increasing the electrical resistance of the device. In addition, before acetone exposure, as the sensor temperature increases in dry air, the oxygen molecules adsorbed on the surface of the sensor trap free electrons [18]. At room temperature the oxygen form is O<sub>2</sub>; while at 100 °C molecules trap one free electron, leading

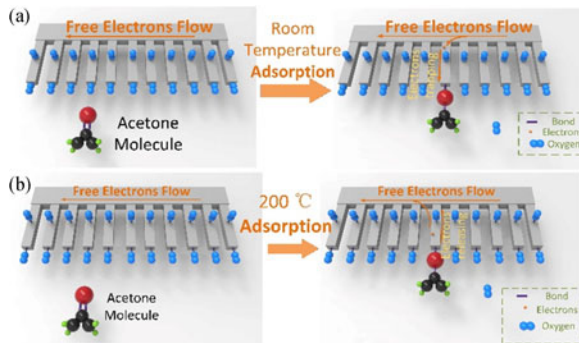


Fig. 7. (a) Adsorption of acetone at room temperature. (b) Adsorption of acetone at 200 °C.

to a mixture of  $O_2$  and  $O_2^-$ . Finally, at 200 °C, almost all the oxygen molecules turn into  $O_2^-$  after each trapping one electron.

In our experiments, the acetone concentration is much lower than that of oxygen and the testing temperature is lower than the autoignition temperature (465 °C) so that oxidation of the acetone will not occur except on the surface. The interaction between sensor surface and acetone initially involves the replacement of adsorbed oxygen molecules on the surface of the sensor. At room temperature the oxygen of the carbonyl group of acetone could displace an adsorbed neutral  $O_2$  molecule as shown in Fig. 7(a). At progressively higher temperatures, the reaction of acetone to form the enol will be favoured (there is predicted [18] to be a 16.4 kJ/mol barrier to this process) and this will result in a stronger bond between the carbonyl oxygen and the surface zinc atom and the formation of a surface O-H bond. These two effects will result in a progressively larger disruption of the conduction band of the ZnO semiconductor leading to an increase in its resistance. At higher temperatures sufficient energy will be available to displace an  $O_2^-$  adsorbed on the surface and also oxidation will start to occur leading to electrons being injected into the conduction band as shown in Fig. 7(b). Thus the sensor response for acetone will show a characteristic temperature dependence. This temperature dependence could be employed as a fingerprint pattern for acetone detection and determination.

## V. CONCLUSION

A nanocomb shaped hierarchical ZnO gas sensor was fabricated using standard MEMS and CVD growth processes. The response of the fabricated ZnO sensor to acetone was analyzed as a function of temperature from 25 °C to 300 °C. The experimental results have shown that the sensor's temperature modulated U-shaped response

constitutes a fingerprint for acetone detection in human breath. The sensor's characteristic response was shown to be linked to the carbonyl group present in the acetone molecule, which results in a change of sensing behavior as the temperature increases.

## ACKNOWLEDGMENT

This work was supported in part by the HK Innovation and Technology Fund ITF under Grant ITS/211/16FP and in part by the Australian Research Council Discovery Projects funding scheme under Project DPI30104374.

## REFERENCES

- [1] U. Jaimini *et al.*, "Investigation of an indoor air quality sensor for asthma management in children," *IEEE Sensors Lett.*, vol. 1, no. 2, Apr. 2017, Art. no. 6000204.
- [2] B. Urasinska-Wojcik and J. W. Gardner, "Identification of  $H_2S$  impurity in hydrogen using temperature modulated metal oxide resistive sensors with a novel signal processing technique," *IEEE Sensors Lett.*, vol. 1, no. 4, Aug. 2017, Art. no. 4500204.
- [3] M. Righettoni, A. Tricoli, and S. E. Pratsinis, "Si:  $WO_3$  sensors for highly selective detection of acetone for easy diagnosis of diabetes by breath analysis," *Anal. Chem.*, vol. 82, no. 9, pp. 3581–3587, 2010.
- [4] Q. Zhang and D. Wang, "Room temperature acetone sensor based on nanostructured  $K_2W_7O_{22}$ ," in *Proc. Int. Conf. IEEE SENSORS*, 2016, pp. 1–3.
- [5] A. Fioravanti *et al.*, "ZnO as functional material for sub-ppm acetone detection," in *Proc. Int. Conf. IEEE SENSORS*, 2014, pp. 803–806.
- [6] J. Luo *et al.*, "The mesoscopic structure of flower-like ZnO nanorods for acetone detection," *Mater. Lett.*, vol. 121, pp. 137–140, 2014.
- [7] A. Rydosz *et al.*, "Performance of Si-doped  $WO_3$  thin films for acetone sensing prepared by glancing angle DC magnetron sputtering," *IEEE Sensors J.*, vol. 16, no. 4, pp. 1004–1012, Feb. 2016.
- [8] S. Kim, S. Park, S. Park, and C. Lee, "Acetone sensing of Au and Pd-decorated  $WO_3$  nanorod sensors," *Sens. Actuators B, Chem.*, vol. 209, pp. 180–185, 2015.
- [9] B. Rao Bhooloka, "Zinc oxide ceramic semi-conductor gas sensor for ethanol vapour," *Mater. Chem. Phys.*, vol. 64, no. 1, pp. 62–65, 2000.
- [10] M. Hjiri, L. El Mir, S. G. Leonardi, N. Donato, and G. Neri, "CO and  $NO_2$  selective monitoring by ZnO-based sensors," *Nanomaterials*, vol. 3, no. 3, pp. 357–369, 2013.
- [11] Y. Zhang, K. Yu, D. Jiang, Z. Zhu, H. Geng, and L. Luo, "Zinc oxide nanorod and nanowire for humidity sensor," *Appl. Surface Sci.*, vol. 242, no. 1, pp. 212–217, 2005.
- [12] X. Pan, X. Zhao, J. Chen, A. Bermak, and Z. Fan, "A fast-response/recovery ZnO hierarchical nanostructure based gas sensor with ultra-high room-temperature output response," *Sens. Actuators B, Chem.*, vol. 206, pp. 764–771, 2015.
- [13] J. Chen, X. Pan, F. Boussaid, A. Bermak, and Z. Fan, "A hierarchical ZnO nanostructure gas sensor for human breath-level acetone detection," in *Proc. Int. Symp. IEEE Circuits Syst.*, 2016, pp. 1866–1869.
- [14] C. Shao *et al.*, "High performance of nanostructured ZnO film gas sensor at room temperature," *Sens. Actuators B, Chem.*, vol. 204, pp. 666–672, 2014.
- [15] J. Gao and A. V. Teplyakov, "Chemical transformations of acetone on ZnO powder," *J. Catalysis*, vol. 319, pp. 136–141, 2014.
- [16] Z. Fan *et al.*, "ZnO nanowire field-effect transistor and oxygen sensing property," *Appl. Phys. Lett.*, vol. 85, no. 24, pp. 5923–5925, 2004.
- [17] [Online]. Available: [https://www.chem.wisc.edu/deptfiles/chem343-esselman/web/mo/job\\_177004.html](https://www.chem.wisc.edu/deptfiles/chem343-esselman/web/mo/job_177004.html). Accessed Apr. 27, 2017.
- [18] N. Yamazoe, J. Fuchigami, M. Kishikawa, and T. Seiyama, "Interactions of tin oxide surface with  $O_2$ ,  $H_2O$  and  $H_2$ ," *Surface Sci.*, vol. 86, pp. 335–344, 1979.